Materials Research. 2015; 18(Suppl 2): 273-278
DOI: http://dx.doi.org/10.1590/1516-1439.371614

Study of the Efficiency of Polypyrrole/ZnO Nanocomposites as Additives in Anticorrosion Coatings

Demétrius Perrelli Valença[a], Kleber Gonçalves Bezerra Alves[a],

Celso Pinto de Melo[b], Nadège Bouchonneau[a]*

[a]Departamento de Engenharia Mecânica, Centro de Tecnologia e Geociências, Universidade Federal de Pernambuco – UFPE, Av. Prof. Moraes Rego, 1235, Cidade Universitária, CEP 50670-901, Recife, PE, Brazil
[b]Departamento de Física, Centro Ciências Exatas e da Natureza, Universidade Federal de Pernambuco – UFPE, Av. Prof. Moraes Rego, 1235, Cidade Universitária, CEP 50670-901, Recife, PE, Brazil

Received: December 15, 2014; Revised: August 30, 2015

We synthesized (ZnO nanoparticles)/polypyrrole (ZnO_NPs/PPy) hybrid nanocomposites and used them as additives in an epoxy paint to protect SAE 1020 carbon steel from corrosion. The nanocomposites were obtained by chemical polymerization of pyrrole in aqueous solution and sodium dodecyl sulfate solution containing dispersed ZnO nanoparticles. We characterized the nanoparticles by infrared absorption spectrophotometry, X-ray diffraction (XRD), scanning electron microscopy (SEM) and transmission electron microscopy (TEM). A large disparity in the distribution of ZnO particle sizes became evident from the TEM images, which also show the formation of hybrid nanocomposites consisting of polypyrrole coated ZnO nanoparticles. Electrochemical impedance spectroscopy (EIS) and open circuit potential (OCP) tests, which were performed on SAE 1020 carbon steel plates coated with epoxy and ZnO_NPs/PPy, have shown that epoxy paints have their efficiency as anticorrosive coatings significantly improved when ZnO_NPs/PPy hybrid nanocomposites are added to them.

Keywords: *corrosion, conducting polymers, nanocomposites, polypyrrole, zinc oxide*

1. Introduction

The degradation of metal surfaces due to atmospheric corrosion is a major problem for many exposed metallic structures, such as bridges, pipelines and storage tanks. If seawater is present, there is a remarkable increase in the degree of corrosion since the environment becomes even more aggressive[1].

Corrosion costs are very high and some studies show that a fifth of the world's steel production is destined to replace losses caused by corrosion. The overall cost of all types of corrosion and its prevention is estimated between 2% and 4% of the GNP (Gross National Product)[2].

The corrosive action of the atmosphere depends primarily on factors such as relative humidity, pollutants, temperature and residence time of electrolyte solutions on the metal surface. The physicochemical characteristics that may interfere with the corrosive action of the environment are the presence of water, salts, gases, differences in pH and electrical conductivity[3]. On the other hand, the corrosion process in metal exposed to soil is mainly due to the natural soil conditions, and not to small variations that may exist in the environment.

Among the methods of corrosion protection, one of the most used is the application of anti-corrosion coatings, which provide a physical barrier between the base metal to be protected and the corrosive environment[4].

The use of zinc as an anticorrosive agent in paints is often adopted as a way to improve the corrosion resistance of metallic components, and these types of coatings can act as a physical barrier while offering galvanic protection[5,6].

Treatment with chromium and phosphate can be used to prolong the lifetime of zinc coatings[7,8].

However, the leaching of such compounds in coatings may cause serious ecological damage, and that encourages the development of corrosion inhibitor compounds that could be less impacting for the environment. Conductive polymers, such as polyaniline (PANI) and polypyrrole (PPy), are organic compounds that usually have a good corrosion stability when in contact with solution or/and in the dry state[9]. They also are a possible answer to the demand for "green" corrosion inhibitors to minimize the health risk to humans and damage to the environment[10-12].

Among the metallic oxides, the zinc oxide (ZnO) has received considerable interest in the production of hybrid materials with polypyrrole due to its variety of applications in optoelectronic devices and anti-corrosion properties. The zinc oxide has high refractive index and thermal stability, UV protection, good transparency and presents high electron mobility. These properties are used in emerging applications

*e-mail: nadege.bouchonneau@gmail.com

where polypyrrole is added as anticorrosive additive for steel coating[13-15].

Our interest aims the development of new anti-corrosive additives to protect carbon steel; more specifically, we want to investigate the efficiency of the addition of new (ZnO /Polypyrrole) hybrid nanoparticles to an organic matrix upon the protection against the corrosion of carbon steel substrates[16].

We describe the synthesis of ZnO_NPs/PPy nanocomposites and their characterization by use of several techniques, such as infrared spectroscopy (FT-IR), X-ray diffraction (XRD), scanning electron microscopy (SEM) and transmission electron microscopy (TEM). Epoxy paint was used as a binder for the nanocomposites so as to obtain more uniform coatings. Then, in order to study the effect of ZnO_NPs/PPy on the corrosion inhibition performance of the epoxy coatings in 3% saline solution at room temperature, coatings were investigated by electrochemical impedance spectroscopy (EIS) and open circuit potential (OCP). In this paper we present and discuss a first assessment of the potential of ZnO_NPs/PPy nanocomposites to be used as anticorrosive pigments.

2. Experimental

2.1. Materials

Pyrrole monomer (C_4H_5N - Sigma-Aldrich, USA) was previously distilled under vacuum and subsequently stored in a dark refrigerated environment (0 °C), since it is a very sensitive to light and moisture. All chemical reagents, such as zinc oxide (ZnO - Mknano, Canada), ferric chloride hexahydrate ($FeCl_3.6H_2O$ - Merk, Brazil) and sodium dodecyl sulfate ($C_{12}H_{25}NaO_4S$ - Sigma-Aldrich, USA), were of analytical grade. PA methanol used in this study was from Merk (Brazil).

2.2. Preparation of ZnO / PPy composites

ZnO / PPy composites were obtained by *in situ* emulsion polymerization of pyrrole in an aqueous solution containing sodium dodecyl sulphate (SDS)[17] and ZnO_NPs. Initially, an aqueous solution of deionized water (40 mL) containing the surfactant (SDS, 2.4 mMoles) was prepared. The solution was stirred vigorously for 10 minutes and 0.5 mMoles of pyrrole monomer were then added to the mixture. After 20 minutes of vigorous stirring, 42.1 µMoles of ZnO were added. Subsequently, the solution was maintained under vigorous stirring for 20 minutes and 400.0 uL of FeCl3 (1M) was added dropwise[1]. Finally, the solution was kept under vigorous stirring for 24 hours to ensure complete polymerization. To obtain a powder composite material, 70 mL of methanol was added to the colloidal dispersion, forming a black precipitate, which was then dried at 40 °C and thoroughly dried in a vacuum desiccator at room temperature.

2.3. Sample characterization

We have used a JSM-5900 (JEOL, Japan) SEM to investigate the morphology of the samples, which were mounted on a small glass slide and covered with a thin gold surface by use of a SDS050 Bal-Tec metallizer (Japan). All TEM observations were performed in a Tecnai G2 Spirit (FEI Company, USA) Transmission Electron Microscope (TEM) with 120 kV at the CpqAM (PDTIS-FIOCRUZ). The samples were deposited in Copper-coated 400 mesh carbon grids. The analysis of vibrational spectroscopy in the infrared region was performed with basis on the use of potassium bromide (KBr) pellets on a FTLA ABB model 2000 FTIR spectrometer (Bomem, Canada) operating in the 4000-400 cm^{-1} region, with a 4 cm^{-1} resolution and by taking 200 accumulations for each spectrum. The crystal structure of the powder was analyzed in a D5000 diffractometer (Siemens AG, Germany) using Cu Kα radiation (λ = 1.542 Å) and nickel filter. The XRD patterns were obtained in the 2θ range from 10 to 70° with 0.02° steps and acquisition time of 1.0 s per step, at 25 °C.

2.4. Preparation of ZnO_NPs/PPy incorporated epoxy paint

SAE 1020 carbon steel specimens of size 50 mm × 50 mm × 3 mm were sandblasted (Sa $2^{1/2}$ standard) and then coated with the developed paint. A commercial epoxy-based paint was used and tested with and without the addition of 0.2%, 0.5% and 1.0% w/w ZnO_NPs/PPy composites. The coatings were applied over the sand blasted steel surfaces using a gravity feed spray gun and average pressure between 5.5 to 6.0 $kgf.cm^{-2}$ and evaluated after 10 days of curing at room temperature. The thickness of the coatings was evaluated using a measurement device (Mitutoyo, Digi-derm version) for ferrous substrates.

Other SAE 1020 carbon steel samples used to monitor electrochemical activity of uncoated metal were prepared with dimensions 10 mm × 10 mm × 3 mm. To minimize the effect of crevice corrosion, insulation tape for high adhesion of the 3M Brazil was applied to delimit an of 0.32 cm^2 area of the substrate for exposure to the electrolyte. The samples were ground and polished with diamond paste to 1µm.

The different coating systems studied are summarized as follow: Uncoated metal; Metal + Epoxy paint without ZnO_NPs/PPy composites; Metal + Epoxy paint + 0.2% w/w ZnO_NPs/PPy composites; Metal + Epoxy paint + 0.5% w/w ZnO_NPs/PPy composites; Metal + Epoxy paint + 1.0% w/w ZnO_NPs/PPy composites.

2.5. Evaluation of corrosion resistant properties of the coating by EIS and OCP studies

To evaluate the efficiency of the coatings against SAE 1020 carbon steel corrosion, electrochemical tests were performed, such as Open Circuit Potential (OCP) and Electrochemical Impedance Spectroscopy (EIS), using an aqueous solution of 3 wt% NaCl to simulate the marine electrolyte.

Electrochemical Impedance Spectroscopy (EIS) studies were performed using an AUTOLAB PGSTAT 302N system, at room temperature (24 °C). Experimental data were acquired and processed by Nova 1.7 software. The impedance measurements were carried out over a frequency range of 6 kHz to 40 mHz using a 10 mV amplitude of sinusoidal voltage as perturbing signal. Corrosion cell was equipped with a platinum gauze as counter electrode and Ag/AgCl, saturated KCl as reference electrode. The coated SAE 1020 carbon steel plate was the working electrode.

Open Circuit Potential (OCP) values were measured for uncoated and coated specimens with and without the addition of ZnO_NPs/PPy composites. The initial time is considered after 2 min immersion in the saline solution and OCP values were measured during a 24-hour interval.

The coating layer thickness was (120.88 ± 16.05) µm, which is within the range specified by the manufacturer (75-150 microns) and the whole area of the working electrode to be tested was 11.22 cm^2. The coated samples were immersed continuously in 3 wt% NaCl solution at room temperature in periods of time ranging from 0 to 24 h.

3. Results and Discussion

In Figure 1 we show the morphology of the ZnO nanoparticles and ZnO_NPs/PPy nanocomposites as revealed by SEM, where one can observe the formation of both the nanocomposite as some homogeneous micrometric agglomerates.

In Figure 2 we present images of ZnO_NPs and ZnO_NPs/PPy nanocomposites obtained by TEM. In Figure 2a one can see the presence of ZnO nanoparticles in the form of bats, rods, prismatic particles and particles without well-defined form, and also a great agglomeration of the particles. It is possible to observe a large width in the distribution of particle sizes. In Figure 2b it can be clearly observed the inorganic phase (ZnO_NPs cores) coated with the organic phase (PPy).

The infrared spectra (FTIR) of the ZnO_NPs, PPy and ZnO_NPs/PPy composite are shown in Figure 3. For the ZnO_NPs, the presence of absorption bands at 480 cm^{-1} is observed, which can be attributed to the stretch mode of ZnO[15].

For the ZnO_NPs/PPy composite and PPy, the presence of absorption bands at 2992, 2850 cm^{-1} is observed, which may be attributed to the symmetric and asymmetric stretching of -CH 2 -groups, respectively. The bands obtained at 1557 cm^{-1} and 1463 cm^{-1} correspond to the stretching of C = C bonds and C-C in the pyrrole rings, respectively.

The absorption band observed at 1307 cm^{-1} corresponds to the deformation of C-H bonds. Also for PPy, stretching vibrations of C-H and C-N bonds were observed at 1201 cm^{-1} and 1043 cm^{-1}. The bands observed between 906 cm^{-1} and 674 cm^{-1} can be assigned, respectively, to the ring deformation out of the plane and to the N-H vibration in the polymer[13].

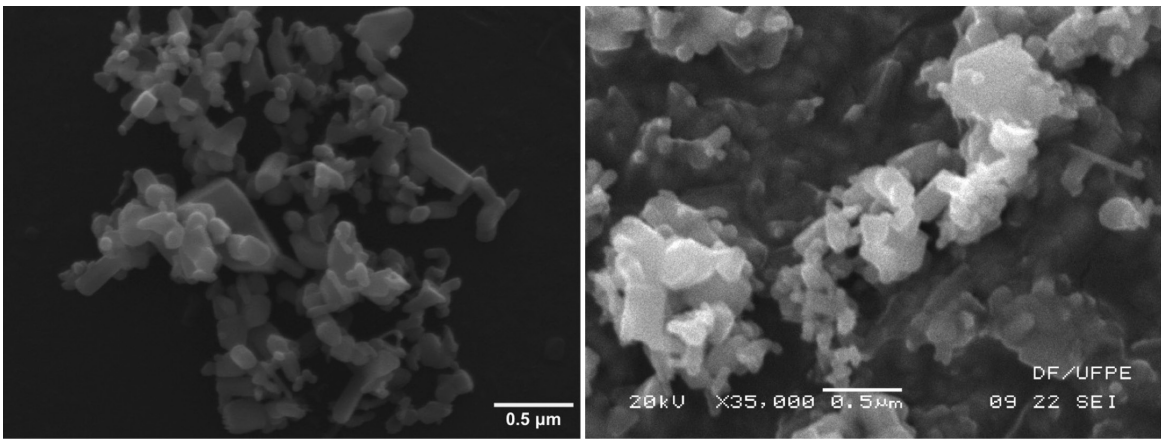

(a) (b)

Figure 1. SEM image of: (a) ZnO_NPs and (b) ZnO_NPs/PPy nanocomposites.

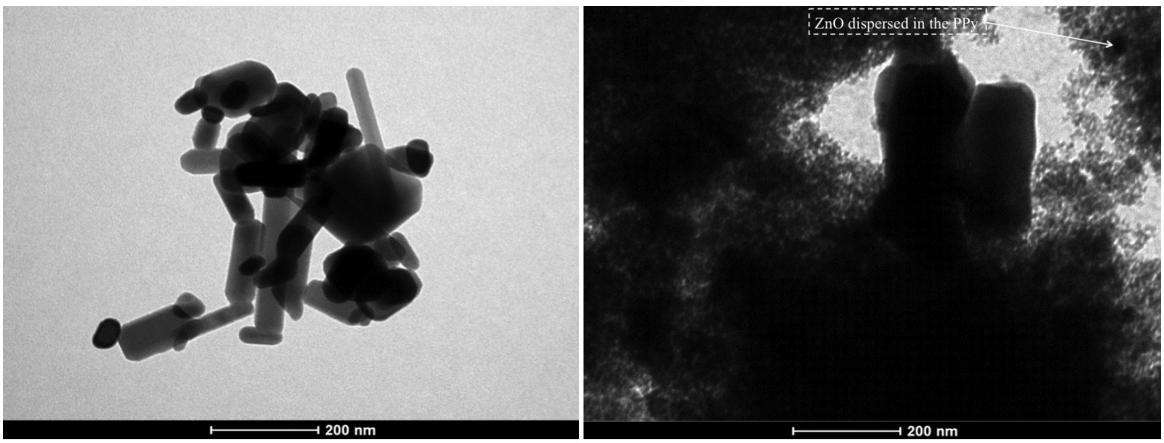

(a) (b)

Figure 2. TEM image of: (a) ZnO_NPs and (b) ZnO_NPs/PPy nanocomposites.

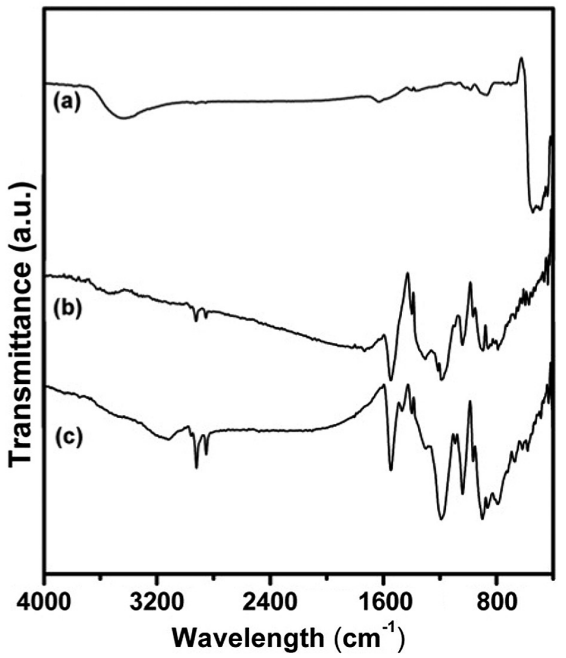

Figure 3. FTIR spectrum of: (a) ZnO_NPs, (b) PPy and (c) ZnO_NPs/PPy.

The infrared spectrum (FTIR) of the ZnO_NPs/PPy nanocomposite did not show the characteristic absorption band of ZnO. This is probably due to the encapsulation of ZnO particle by PPy. Such interpretation has already been introduced in other works, for instance in studies of ZnO_NPs/PANI nanocomposite. The authors Alves et al.[18] stress that they were not able to identify all of the Bragg reflections seen in the pure ZnO_NPs in the X-ray diffractogram of ZnO_NPs/PANI, but only the presence of the 2θ = 31.8° peak (corresponding of the (100) reflections). A similar situation was reported in Tang et al.[19], possibly because the ZnO_NPs are well embedded in a PANI envelope.

Patterns of X-ray diffraction (XRD) analysis found for the ZnO_NPs and the ZnO_NPs/PPy composite are shown in Figure 4. The main diffraction peaks for the ZnO_NPs, which are located at 2θ = 31.8°; 34.4°; 36.2°; 47.5°; 56.6; 62.9°; 66.4°; 67.9 and 69.1° and correspond to Bragg reflections (100), (002), (101) (102) (110) (103) (200) (112) and (201), respectively, allowed us to identify a hexagonal wurzita type structure (a = 3. 25 Å and c = 5.21 Å) for ZnO. These peaks are in agreement with the data obtained for ZnO[20].

By analyzing the results obtained for the ZnO_NPs/PPy composite, we observed a peak at 2θ = 20º, which corresponds to a semicrystalline structure of polypyrrole. The diffraction peaks of ZnO are not observed in the XRD pattern of the composite particle, a fact consistent with the hypothesis that the ZnO particles would be encapsulated by the PPy chains[21].

In Figure 5 we show the OCP results obtained for each coating immersed in a 3 wt% NaCl solution. One can observe that the corrosion protection of all coating systems has been improved when compared to the uncoated metallic substrate. The coating epoxy+ 0.2% w/w nanocomposite

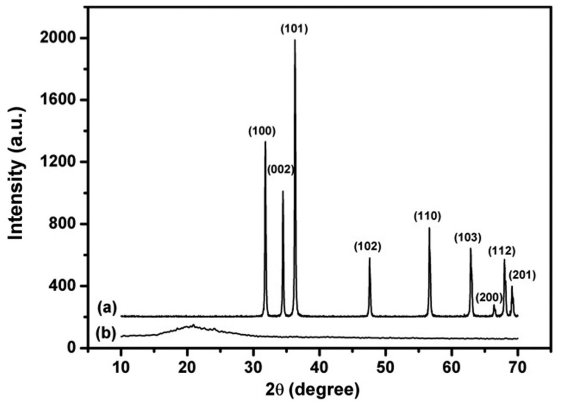

Figure 4. X-ray diffraction patterns obtained for: (a) ZnO (b) ZnO / PPy.

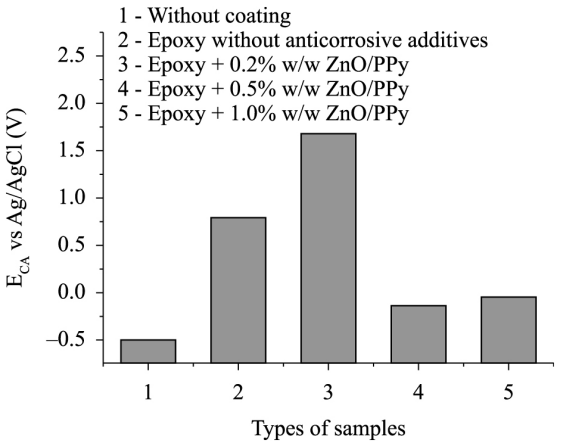

Figure 5. Corrosion potential of coated and uncoated metal obtained by OCP.

showed a particularly great performance relative to the other coating systems.

The anticorrosion performance of the ZnO_NPs/PPy in epoxy coatings on the SAE 1020 carbon steel plate was investigated by EIS measurements in a 3 wt% NaCl solution. In Figure 6 we show the Nyquist plots of the epoxy coatings and the uncoated metal, with and without the addition of ZnO_NPs/PPy, obtained at zero immersion time. The epoxy coating + 0.2% w/w ZnO_NPs/PPy also showed a high impedance value, indicating a great efficiency against corrosion.

The epoxy coating with 0.2% w/w ZnO_NPs/PPy composite showed larger capacitive loops, in an indication that this coating offers a better protection to electrical current than pure epoxy and epoxy +0.5% or 1.0% w/w ZnO _NPs/PPy. This could be associated to an increased porosity of particles by effect of agglomeration[17], and thus a higher permeation of the electrolyte through the coatings.

To allow for a more detailed study of pure epoxy and epoxy +0.5% or 1.0% w/w ZnO _NPs/PPy curves, a graphic was generated by suppressing the curves of pure epoxy and epoxy + 0.2% w/w ZnO _NPs/PPy, and reordering the scales

Table 1. Resistance obtained at zero immersion time.

Substrate conditions	Without coating	Epoxy without anticorrosive additives	Epoxy +0.2% w/w ZnO/PPy	Epoxy +0.5% w/w ZnO/PPy	Epoxy +1.0% w/w ZnO/PPy
Resistance (10^3Ohm)	52.1	17.5×10^7	50.6×10^7	52.1×10^7	17.9×10^3

(see separated graph in Figure 6). It can be observed that the samples coated with epoxy + 0.5% and + 1.0% w/w ZnO _NPs/PPy have a similar behavior to that of the uncoated sample. This reduction of the protection efficiency may be associated with the increased porosity due to particle agglomeration[22], which allows water to penetrate into the coatings and foster the degradation of the metallic surface by increased exposure to the saline medium.

Resistance values of each system (coated and uncoated) have been obtained from the Nyquist diagrams by extrapolating the capacitive loop to the real axis. The values of resistance obtained at zero immersion time are presented in Table 1.

The fact that at zero immersion time, low resistance values were obtained for both the uncoated metal and metal samples coated with epoxy+ 1.0% w/w nanocomposites, reveal an intense permeation of the electrolyte, even at the beginning of the immersion tests. On the other hand, the coating capacitance is associated with water absorption in the coating so that it can be used as a very important parameter for assessing the behavior of a coating over time. Therefore, capacitance measurements allow a better understanding of the permeability of an organic coating[23,24].

In Figure 7 we represent the evolution of the capacitance versus exposure time for all systems studied. The results show that the capacitance value increases during the first hours of exposure to the electrolyte, and that, after a slight variation they tend to stabilize. When freshly immersed in aqueous solutions, organic coatings generally exhibit a moderate increase in capacitance values, which stops when the coating film becomes saturated[25]. This increase in the capacitance values illustrates the permeation of the electrolyte through the organic coating, which occurs during exposure to saline solution. When the electrolyte permeates the coating, the capacitance is typically in the range between 10^{-8} to 10^{-10} F. With increasing immersion times, the capacitance can reach values around 10^{-7} to 10^{-4} F at more advanced stages[26].

The epoxy+0.2% w/w nanocomposites coating presents capacitance values of about 10^{-10} F at zero immersion time. After 24h exposition, the capacitance values reached approximately and 2.5×10^{-10} F, suggesting the permeation of the electrolyte.

These preliminary tests demonstrate that, as expected, the addition of ZnO_NPs/PPy contributed to a better anticorrosive protection of epoxy coatings. This offers promising possibilities for the development of ZnO_NPs/PPy additives for anticorrosive paints. Our research group is now implementing further tests adopting several exposure times to saline media and higher filler concentrations, in order to evaluate the efficiency of each organic coating as a function of time and the amount of hybrid nanocomposites added.

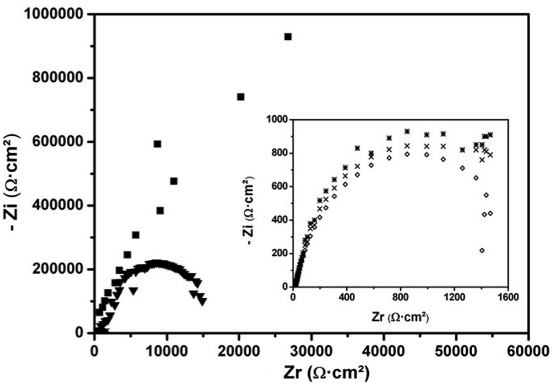

Figure 6. Nyquist diagram for: (◊) uncoated metal; samples coated with epoxy: (▼) without anticorrosive additives, (■) +0.2%, (×) +0.5% and (*) +1.0% w/w ZnO/PPy.

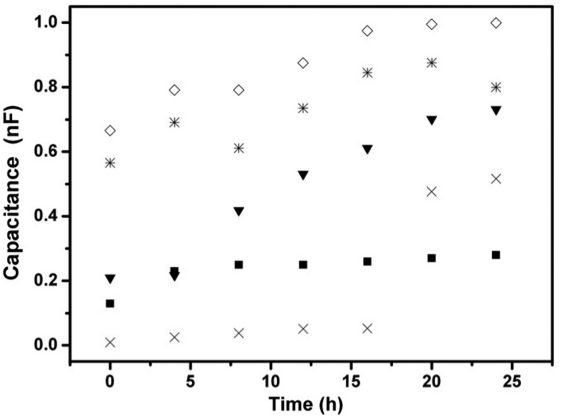

Figure 7. Capacitance values obtained during 24h immersion in saline solution for: (◊) uncoated metal; samples coated with epoxy: (▼) without anticorrosive additives, (■) +0.2%, (×) +0.5% and (*) +1.0% w/w ZnO/PPy.

4. Conclusions

In the present work, we report the synthesis of ZnO_NPs/PPy nanocomposites obtained by polymerization of pyrrole in presence of SDS and ZnO_NPs. TEM images have confirmed the hypothesis that the prepared ZnO_NPs exhibit a large distribution of particle sizes and that the ZnO_NPs/PPy nanocomposites are composed by ZnO cores enveloped with polypyrrole chains. Finally, EIS measurements show that ZnO_NPs/PPy coated metal samples presented higher corrosion resistance when compared to the uncoated ones. Particularly, the addition of the 0.2% w/w ZnO_NPs/PPy

nanocomposites to the epoxy paint allows a greater anticorrosive efficiency, when compared to pure epoxy paint without any corrosion inhibitor. This behavior might be further exploited for the development of innovative hybrid nanopigments for corrosion protection. Coatings with higher percentages of nanocomposites presented lower protection efficiency, a result that could be attributed to the increased porosity of the coating due to particles agglomeration. Electrochemical impedance spectroscopy and open circuit potential tests also proved to be very sensitive to electrolyte permeation through the coatings, which was observed with the increase of the capacitance during exposure time.

Acknowledgements

This work was supported by the Brazilian agency CAPES. The authors would like to thank the Program for Technological Development in Tools for Health-PDTIS-FIOCRUZ for the Electron Microscopy Service-CPqAM facilities and Profs. S. L. Urtiga Filho, M. R. S. Veira and L. R. R. Barbosa (UFPE) for the EIS measurements.

References

1. Baere K, Verstraelen H, Rigo P, Van Passel S, Lenaerts S and Potters G. Reducing the cost of ballast tank corrosion: an economic modeling approach. *Marine Structures*. 2013; 32:136-152. http://dx.doi.org/10.1016/j.marstruc.2013.02.003.
2. Ropital F. *Corrosion and degradation of metallic materials: understanding of the phenomena and applications in petroleum and process industries*. Paris: Editions Technip; 2010. 276 p.
3. Picon CA, Fernandes FAP, Tremiliosi-Filho G, Rodrigues CAD and Casteletti LC. Estudo do mecanismo de corrosão por pites em água do mar de aços inoxidáveis supermartensíticos microligados com Nb E Ti. *Revista Escola de Minas*. 2010; 63(1):65-69. http://dx.doi.org/10.1590/S0370-44672010000100011.
4. Gentil V. *Corrosão*. 6th ed. Rio de Janeiro: Livros Técnicos e Científicos; 2011.
5. Hammouda N, Chadli H, Guillemot G and Belmokre K. The corrosion protection behaviour of zinc rich epoxy paint in 3% NaCl solution. *Advances in Chemical Engineering and Science*. 2011; 1(2):51-60. http://dx.doi.org/10.4236/aces.2011.12009.
6. Shi H, Liu F and Han EH. The corrosion behavior of zinc-rich paints on steel: Influence of simulated salts deposition in an offshore atmosphere at the steel/paint interface. *Surface and Coatings Technology*. 2011; 205(19):4532-4539. http://dx.doi.org/10.1016/j.surfcoat.2011.03.118.
7. Hihara LH, Adler RPI, Latanision RM, editors. *Environmental degradation of advanced and traditional engineering materials*. Boca Raton: CRC Press; 2013. 719 p. http://dx.doi.org/10.1201/b15568.
8. Tomachuk CR, Sarli AR and Elsner CI. Anti-corrosion performance of Cr+6-free passivating layers applied on electrogalvanized. *Materials Sciences and Applications*. 2010; 1(4):202-209. http://dx.doi.org/10.4236/msa.2010.14032.
9. Riccardis MF and Martina V. Hybrid conducting nanocomposites coatings for corrosion protection. In: Aliofkhazraei M, editor. *Developments in corrosion protection*. Rijeka: InTech; 2014. p. 271-317.http://dx.doi.org/10.5772/57278.
10. Sitaram SP, Stoffer JO and O'Keefe TJ. Application of conducting polymers in corrosion protection. *Journal of Coatings Technology*. 1997; 69(866):65-69. http://dx.doi.org/10.1007/BF02696146.
11. Branzoi V, Pruna A and Branzoi F. Inhibition effects of some organic compounds on Zinc corrosion in 35% NaCl. *Revista de Chimie*. 2008; 59(5):540-554.
12. Pan T. Intrinsically conducting polymer-based heavy-duty and environmentally friendly coating system for corrosion protection of structural steels. *Spectroscopy Letters*. 2013; 46(4):268-276. http://dx.doi.org/10.1080/00387010.2012.725235.
13. Batool A, Kanwal F, Imran M, Jamil T and Siddiqi SA. Synthesis of polypyrrole/zinc oxide composites and study of their structural, thermal and electrical properties. *Synthetic Metals*. 2012; 161(23-24):2753-2758. http://dx.doi.org/10.1016/j.synthmet.2011.10.016.
14. Lehr IL and Saidman SB. Anticorrosive properties of polypyrrole films modified with Zinc onto SAE 4140 steel. *Progress in Organic Coatings*. 2013; 76(11):1586-1593. http://dx.doi.org/10.1016/j.porgcoat.2013.07.004.
15. Wang ZL. Nanostructures of zinc oxide. *Materials Today*. 2004; 7(6):26-33. http://dx.doi.org/10.1016/S1369-7021(04)00286-X.
16. Jagtap RN, Patil PP and Hassan SZ. Effect of zinc oxide in combating corrosion in zinc-rich primer. *Progress in Organic Coatings*. 2008; 63(4):389-394. http://dx.doi.org/10.1016/j.porgcoat.2008.06.012.
17. Melo EF, Alves KGB, Junior SA and Melo CP. Synthesis of fluorescent PVA/polypyrrole-ZnO nanofibers. *Journal of Materials Science*. 2013; 48(10):3652-3658. http://dx.doi.org/10.1007/s10853-013-7159-2.
18. Alves KGB, Felix JF, Melo EF, Santos CG, Andrade CAS and Melo CP. Characterization of ZnO/Polyaniline nanocomposites prepared by using surfactant solutions as polymerization media. *Journal of Applied Polymer Science*. 2012; 125(S1):E141-E147. http://dx.doi.org/10.1002/app.35502.
19. Tang BZ, Geng YH, Sun QH, Zhang XX and Jing XB. Processible nanomaterials with high conductivity and magnetizability. preparation and properties of maghemite/polyaniline nanocomposite films. *Pure and Applied Chemistry*. 2000; 72(1-2):157-162. http://dx.doi.org/10.1351/pac200072010157.
20. Shao H, Qian XF and Huang BC. Fabrication of singlecrystal ZnO nanorods and ZnS nanotubes through a simple ultrasonic chemical solution method. *Materials Letters*. 2007; 61(17):3639-3643. http://dx.doi.org/10.1016/j.matlet.2006.12.005.
21. Alves KGB, Felix JF, Melo EF, Santos CG, Andrade CAS and Melo CP. Characterization of ZnO/Polyaniline nanocomposites prepared by using surfactant solutions as polymerization media. *Journal of Applied Polymer Science*. 2011; 125(S1):E141-E147. http://dx.doi.org/10.1002/app.35502.
22. Jinhai W, Xu H, Battocchi D and Bierwagen G. The determination of critical pigment volume concentration (cpvc) in organic coatings with fluorescence microscopy. *Progress in Organic Coatings*. 2014; 77(12 part B):2147-2154. http://dx.doi.org/10.1016/j.porgcoat.2013.12.010.
23. Amirudin A and Thierry D. Application of electrochemical impedance spectroscopy to study the degradation of polymer: coated metals. *Progress in Organic Coatings*. 1995; 26(1):1-28. http://dx.doi.org/10.1016/0300-9440(95)00581-1.
24. Penon MG, Picken SJ, Wübbenhorst M, de Vos G and van Turnhout J. Dielectric water sorption analysis. *The Review of Scientific Instruments*. 2006; 77(11):115107. http://dx.doi.org/10.1063/1.2370739.
25. Deflorian F, Fedrizzi L, Rossi S and Bonora PL. Organic coatings capacitance measurement by EIS: ideal and actual trends. *Electrochimica Acta*. 2009; 44(24):4243-4249. http://dx.doi.org/10.1016/S0013-4686(99)00139-5.
26. Wolynec S. *Técnicas eletroquímicas em corrosão*. São Paulo: EDUSP; 2003.